

Electronic Supplementary Information

**Broadband White-Light Emission in a One-Dimensional Organic
–Inorganic Hybrid Cadmium Chloride with Face-Sharing CdCl₆
Octahedral Chains†**

Zhikai Qi,^a Yali Chen,^a Yao Guo,^b Xuelian Yang,^a Fu-Qiang Zhang,^a Guojun Zhou,^a
and Xian-Ming Zhang^{a,*}

^a*Key Laboratory of Magnetic Molecules & Magnetic Information Materials (Ministry of Education), Institute of Chemistry and Culture, School of Chemistry & Material Science, Shanxi Normal University, Linfen 041004, P. R. China.*

Email: zhangxm@dns.sxnu.edu.cn; Tel: +86-357-2051402

^b*Henan Joint International Research Laboratory of Nanocomposite Sensing Materials, School of Chemical and Environmental Engineering, Anyang Institute of Technology, Anyang 455000, China*

1. Methods

1.1 Characterization. Digital microscope (HiROX RH-2000, Japan) was used to acquire photograph of (2cepiH)CdCl₃ crystal. Fourier transform infrared (FT-IR) spectra of (2cepiH)CdCl₃ were recorded from KBr pellets in range 400-4000 cm⁻¹ on a Nicolet iS50 spectrometer. Thermogravimetric analysis (TGA) was carried out on a NETZSCH STA 449F3 thermal analyzer under N₂ at a heating rate of 10 °C/min. Powder X-ray diffraction (XRD) measurements were measured at 40 kV and 100 mA on a Rigaku D/Max-2500 diffractometer with Cu K α radiation, and the powder diffraction patterns were collected in the 2 θ range of 5° to 50° with a step size of 0.02 min⁻¹. The Raman spectra were performed on the bulk crystal of (2cepiH)CdCl₃ in the range of 100-3000 cm⁻¹ using a micro Raman confocal microscope under 785 nm excitation wavelength.

1.2 Photocurrent Measurements. Electrode of (2cepiH)CdCl₃ was prepared by a solution coating method to conduct photocurrent measurement. 5 mg of (2cepiH)CdCl₃ powder was firstly dispersed in 100 μ L of ethanol and 10 μ L of Nafion solution (5 wt.%, Sigma-Aldrich), and fully mixed through 10 min of ultrasonication. Then, 40 μ L of suspension is carefully dropped onto a cleaned indium-tin oxide glass substrate (1 \times 1 cm²) and exposed to the air for 2h. A complete and uniform coating can be obtained and used as the work electrode. Photocurrent measurements were carried out in a three-electrode system by the CHI 760E electrochemical workstation, in which Ag/AgCl electrode and Pt plate are used as reference and auxiliary electrodes, respectively, and the electrolyte is aqueous solution of Na₂SO₄ (0.2 M). Moreover, all experiments were performed at a bias potential of +0.4 V, and the full-wavelength light source (300 W high-pressure xenon lamp) is placed about 20 cm away from the work electrode. During cycle test, the irradiation switching intervals are 20 s.

2. Supporting figures

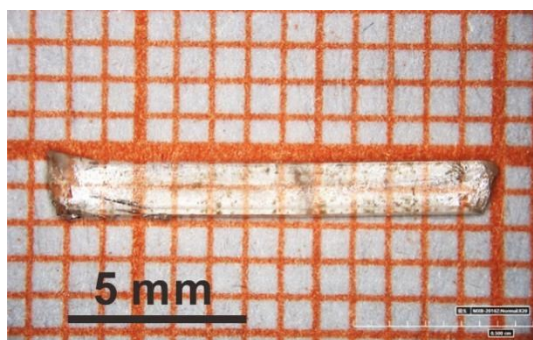


Figure S1. Photograph of (2cepiH)CdCl₃ crystal.

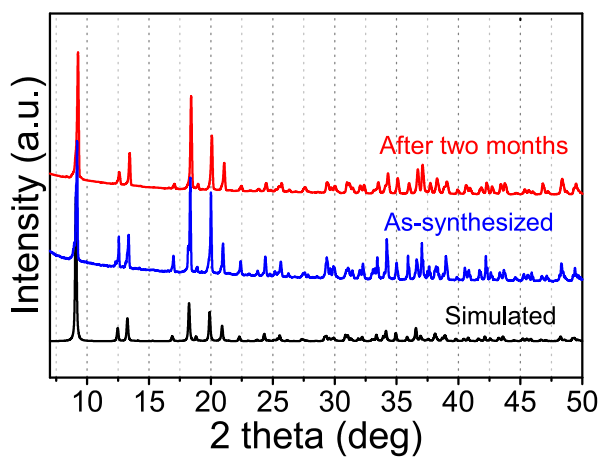


Figure S2. Experimental and simulated powder XRD data of (2cepiH)CdCl₃.

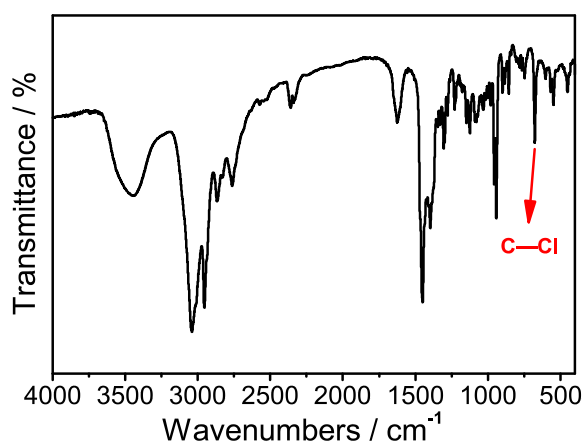


Figure S3. FT-IR spectrum of (2cepiH)CdCl₃ with a sharp peak at 674 cm⁻¹ corresponding to the C-Cl stretching vibration.

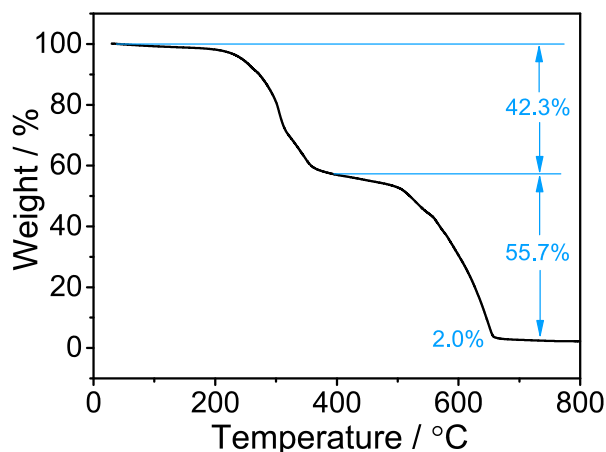


Figure S4. TGA curve of (2cepiH)CdCl₃.

The TGA curve of (2cepiH)CdCl₃ exhibits two distinct weight loss steps in the temperature range from 200 to 664°C. With the increasing temperature, the weight loss occurs until to 200 °C, which shows that (2cepiH)CdCl₃ has a high thermal stability. Then, the first weight loss of 42.3% in 200 – 396°C corresponds to the elimination of organic cations (2cepiH)⁺ (calcd. 40.5%), and the second weight loss is about 55.7% assigned to the removal of inorganic polyanions [CdCl₃]_n⁻ chains (calcd. 59.5%). The remnant weight is only 2% after 664 °C, which may stem from the error in the instrument.

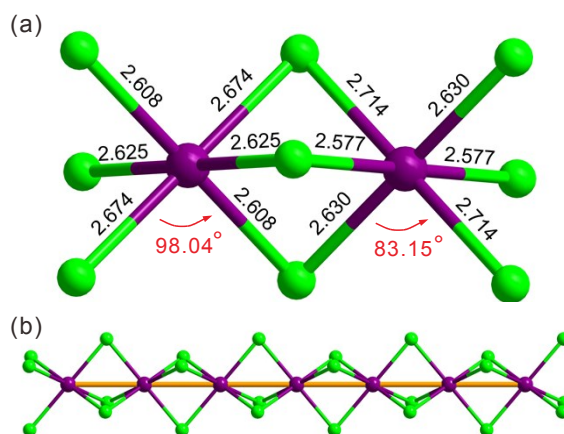


Figure S5. (a) All of Cd-Cl bond lengths and typical Cl–Cd–Cl bond angles in **1**. (b) 1D inorganic infinite [CdCl₃]_n⁻ chain composed of face-sharing CdCl₆ octahedra, where all of the Cd atoms are arranged along a straight line.

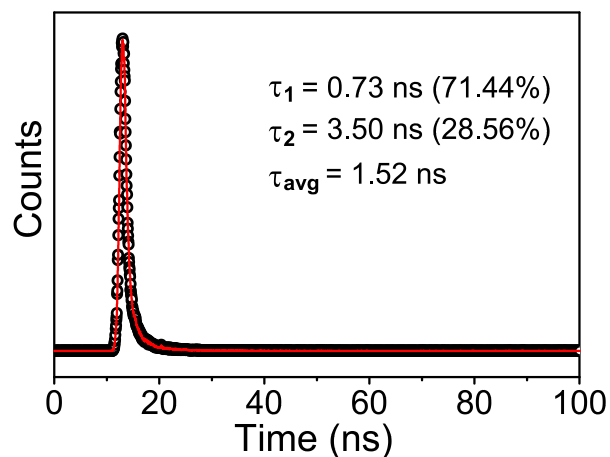


Figure S6. Time-resolved photoluminescence decay and fitting of **1** at 451 nm.

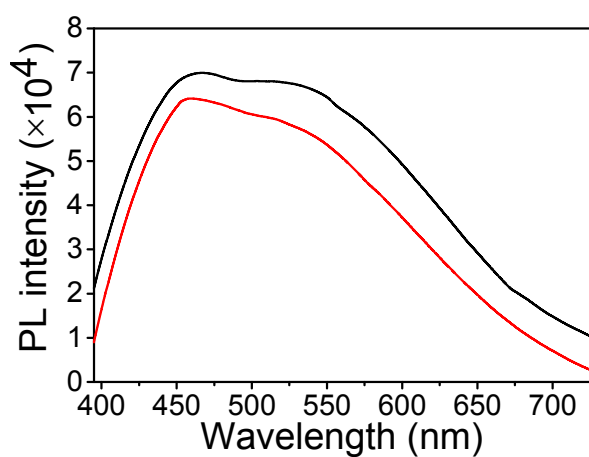


Figure S7. Emission spectra of $(2\text{cepiH})\text{CdCl}_3$ before (black line) and after (red line) about two months.

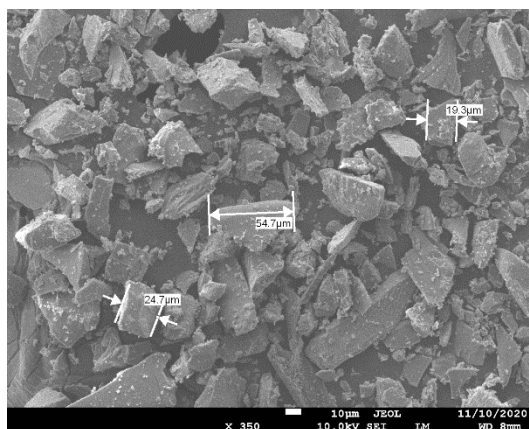


Figure S8. SEM image of μm -sized particles of $(2\text{cepiH})\text{CdCl}_3$.

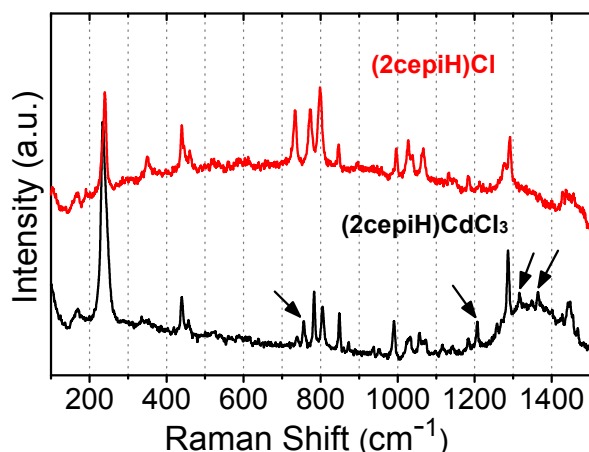


Figure S9. Raman spectra of (2cepiH)Cl and (2cepiH)CdCl₃.

As shown in Figure S9, active modes of (2cepiH)Cl and (2cepiH)CdCl₃ were examined by using Raman spectroscopy. The red curves shows the spectral features belong to pure vibrational modes of the organic molecules, while the black arrows indicate new active modes of (2cepiH)⁺ embedded in the metal halide framework. This result proves the presence of a great intermolecular interaction between organic and inorganic parts, which probably brings about the structural distortion of inorganic octahedral units.

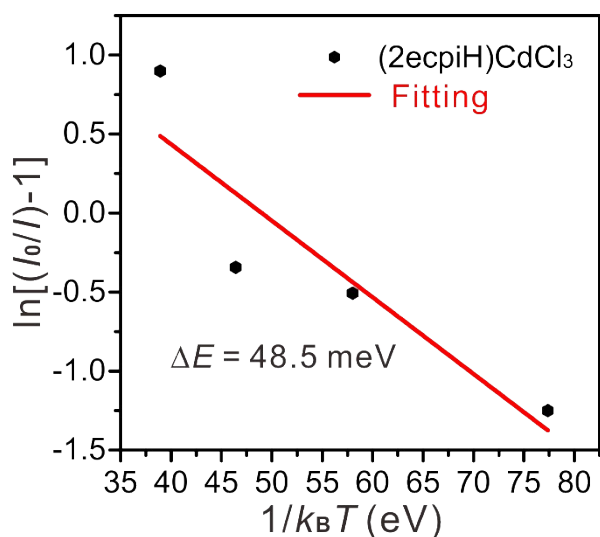


Figure S10. Calculated the STE binding energy as a function of Arrhenius equation.

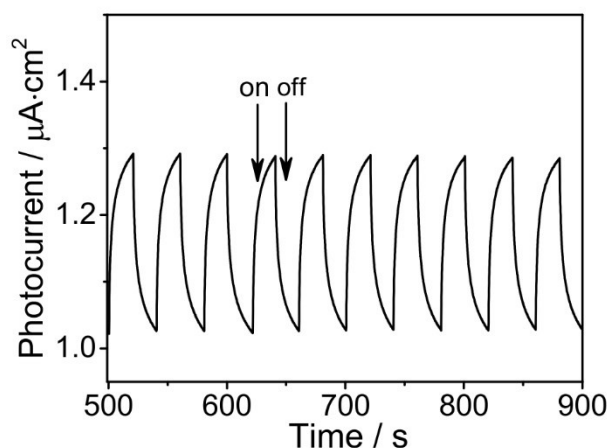


Figure S11. Photocurrent responses of (2cepiH)CdCl₃ under repetitive irradiation.

It is known that photoexcitation with photo energies above the band gap leads to the separation of photo-generated carriers (electrons and holes) inside the semiconductor, allowing for the catalysis behaviors in various reactions. The photocatalysis capability is closely related to the charge-separation efficiency for semiconductor materials. Our experimental and calculated results reveal that (2cepiH)CdCl₃ is a semiconductor. Therefore, we perform the transient short-circuit photocurrent tests to examine the charge-separation efficiency (see Methods for details). Figure S11 shows that (2cepiH)CdCl₃ possesses clear photocurrent responses, although the samples can be partially solved in the electrolyte. Specifically, upon illumination, the photocurrents were quickly generated without an obvious intensity decrease, while the photocurrents rapidly decayed as the light was switched off. This indicates the good photo-electric response and high photophysical stability of (2cepiH)CdCl₃.

3. Supporting tables

Table S1. Crystal data of **1**

Compound	1
Formula	C ₇ H ₁₅ NCdCl ₄
Mr	367.41
<i>T</i> /K	150
Crystal system	monoclinic
Space group	<i>P</i> 2 ₁ / <i>c</i>
<i>Z</i>	4
<i>a</i> /Å	6.7183(2)
<i>b</i> /Å	13.2093(4)
<i>c</i> /Å	14.8063(4)
α /°	90
β /°	107.673(2)
γ /°	90
<i>V</i> /Å ³	1251.96(6)
ρ_{calc} /gcm ⁻³	1.949
μ /mm ⁻¹	2.556
<i>F</i> (000)	720.0
Size/mm ³	0.5×0.2×0.2
<i>T</i> _{max} / <i>T</i> _{min}	1.000/0.853
<i>S</i>	1.152
<i>R</i> _{int} / <i>R</i> _{sigma}	0.0332/0.0299
Reflections	9126/2208
Data/Para.	1853/121
<i>R</i> ₁ ^a , <i>wR</i> ₂ ^b [<i>I</i> >2σ(<i>I</i>)]	0.0293/0.0752
<i>R</i> ₁ ^a , <i>wR</i> ₂ ^b (all data)	0.0369/0.0804
$\Delta\rho_{\text{max}}/\Delta\rho_{\text{min}}$ / e Å ⁻³	0.48/-1.52
CCDC No.	2011052

$$^a R_1 = \sum ||F_o| - |F_c|| / \sum |F_o|. \quad ^b wR_2 = [w(F_o^2 - F_c^2)^2 / w(F_o^2)^2]^{1/2}$$

Table S2. Selective bond lengths and bond angles.

Atom–Atom	Length / Å	Atom–Atom	Length / Å
Cd1...Cd2a	3.3592	Cd2...Cd1d	3.3591
Cd1...Cd2	3.3591	Cd2–Cl1c	2.7145(8)
Cd1–Cl1b	2.6740(9)	Cd2–Cl1	2.7145(8)
Cd1–Cl1	2.6740(9)	Cd2–Cl2	2.5771(9)
Cd1–Cl2b	2.6254(8)	Cd2–Cl2c	2.5771(9)
Cd1–Cl2	2.6254(8)	Cd2–Cl3c	2.6302(9)
Cd1–Cl3a	2.6081(9)	Cd2–Cl3	2.6302(9)
Cd1–Cl3c	2.6081(9)	Cl3–Cd1d	2.6080(9)
Atom–Atom–Atom	Angle / °	Atom–Atom–Atom	Angle / °
Cd2–Cd1–Cd2a	180.0	Cl2–Cd2–Cl1	84.12(3)
Cl1–Cd1–Cl1b	180.0	Cl2–Cd2–Cl1c	95.88(3)
Cl2–Cd1–Cl1b	96.00(3)	Cl2–Cd2–Cl1	84.12(3)
Cl2–Cd1–Cl1	84.00(3)	Cl2–Cd2–Cl1	95.88(3)
Cl2b–Cd1–Cl1	96.00(3)	Cl2–Cd2–Cl2	180.0
Cl2b–Cd1–Cl1b	84.00(3)	Cl2–Cd2–Cl3	95.09(3)
Cl2–Cd1–Cl2b	180.0	Cl2–Cd2–Cl3	84.91(3)
Cl3c–Cd1–Cl1	83.15(3)	Cl2–Cd2–Cl3	95.09(3)
Cl3a–Cd1–Cl1b	83.15(3)	Cl2–Cd2–Cl3	84.91(3)
Cl3a–Cd1–Cl1	96.85(3)	Cl3–Cd2–Cl1c	81.96(3)
Cl3c–Cd1–Cl1b	96.85(3)	Cl3c–Cd2–Cl1c	98.04(3)
Cl3c–Cd1–Cl2	84.39(3)	Cl3–Cd2–Cl1	98.04(3)
Cl3c–Cd1–Cl2b	95.61(3)	Cl3c–Cd2–Cl1	81.96(3)
Cl3a–Cd1–Cl2	95.61(3)	Cl3c–Cd2–Cl3	180.0
Cl3a–Cd1–Cl2b	84.39(3)	Cd1–Cl1–Cd2	77.12(2)
Cl3c–Cd1–Cl3a	180.0	Cd2–Cl2–Cd1	80.43(2)
Cl1–Cd2–Cl1c	180.00(3)	Cd1d–Cl3–Cd2	79.77(3)

Symmetric code: (a) -1+x, +y, +z; (b) -1-x, -1-y, -1-z; (c) -x, -1-y, -1-z; (d) 1+x, +y, +z